Enhanced Electromagnetic Energy Harvesting with Subwavelength Chiral Structures

Zhenya Dong, Fengyuan Yang, and John S. Ho[*]

Department of Electrical and Computer Engineering,
National University of Singapore, Singapore 117583, Singapore
(Received 28 July 2017; published 31 October 2017)

Collecting energy from electromagnetic radiation in dynamic environments is challenging because most harvesting structures are sensitive to the orientation of the polarization state. Here, we show that a subwavelength chiral structure can uniformly collect power from all orientations of a polarization state. Engineering the chirality of the structure exchanges the dependency on orientation with a dependency on field helicity, and results in a chiral enhancement effect in a circularly polarized field of the same handedness. We demonstrate enhanced energy harvesting with the chiral structures by wirelessly powering light-emitting devices in a radiative field.

DOI: 10.1103/PhysRevApplied.8.044026

I. INTRODUCTION

Methods for harvesting energy from radio-frequency electromagnetic radiation have received much renewed interest, motivated by applications in wireless powering [1–12]. An integral component in such systems is the harvesting structure, which extracts energy from the incident radiation and delivers it to a load. Early systems used conventional antennas integrated with rectifying circuits for power conversion, but are challenging to miniaturize because the dimensions must be comparable to the wavelength [2]. Recent work has focused on subwavelength structures for both single-element and array-based harvesting systems [4–12]. Although substantial progress has been made in optimizing the spatial and frequency response of these structures, the polarization response has been limited to a characteristic electric or magnetic dipole in which energy is efficiently collected only when the structure is aligned with the orientation angle θ of the incident polarization state. A widely used scheme to circumvent this limitation is to employ circularly polarized radiation, but the collected power is halved for all orientation angles [6]. This sensitivity to polarization limits the performance of energy harvesting systems in dynamic environments where the orientation of the device is variable, such as when powering moving devices or biomedical implants [13,14].

Here, we demonstrate subwavelength structures that collect energy uniformly for all orientations of the incident polarization state. By engineering the chiral response of a subwavelength helix, we show that the dependency on the orientation angle θ can be exchanged with a dependency on helicity χ, which is invariant under rotation. In contrast with nonchiral structures, the energy extracted from a CP field of the same handedness is twice that independently collected from the structure's dipole components. We demonstrate the use of these structures in energy harvesting systems by wirelessly powering light-emitting devices in both a linearly polarized (LP) and CP radiative field.

II. CHIRAL STRUCTURES

An object is electromagnetically chiral if it interacts differently with left- and right-hand CP radiation [15]. In radio-frequency and optical systems, engineering the chiral response of structures has enabled unusual properties such as zero backscattering [16,17], broadband absorption in thin sheets [18], and enhanced selective excitation of chiral molecules [19–22]. The chiral response can be tuned by modifying the magnetoelectric polarizability of a structure, without the need for bulky phase-delay components used in conventional CP detectors and antennas. We use this property to design subwavelength structures that collect energy independently of the orientation of the field polarization.

Figure 1(a) illustrates a radiative field normally incident on a chiral energy harvesting structure. Except when circularly polarized, the field has an orientation θ defined as the angle between the major axis of the polarization ellipse and the axis of the harvesting structure. The axis of the structure is aligned with the vectorial port across which the electrical load is placed and is well defined irrespective of the shape symmetry of the structure. The polarization response of a chiral and nonchiral structure is shown in Fig. 1(b) on the Poincaré sphere. Every point on the sphere corresponds to an incident polarization state whose orientation angle is represented by the azimuthal angle 2θ and helicity by the altitudinal angle 2χ. The response of the nonchiral structure, such as an electric or magnetic dipole, exhibits a strong dependency on θ (null when the field is linearly polarized in a direction orthogonal to the axis of the structure), but no dependency on χ. Chirality exchanges the dependency on orientation θ with a dependency on helicity χ through a $\pi/2$ rotation on the Poincaré sphere. The chiral

[*]johnho@nus.edu.sg

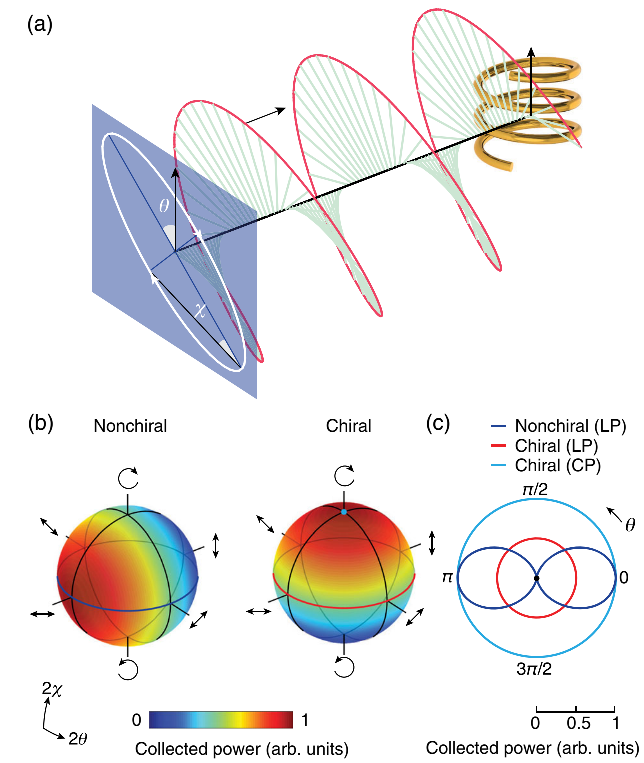

FIG. 1. Polarization response of chiral structures. (a) Electric field component of elliptically polarized radiation normally incident on a harvesting structure. The polarization state has an orientation angle θ relative to the axis of the structure and helicity χ. (b) Response of a chiral and nonchiral structure on the Poincaré sphere. The polarization state is represented by a point on the sphere with azimuthal angle 2θ and altitudinal angle 2χ. (c) Collected power as a function of orientation θ for the chiral and nonchiral structure in a LP field and *CP* field of the same handedness as the structure.

structure collects equal energy for all orientations θ of a particular polarization state, with the maximum occurring when the incident field is circularly polarized with the same helicity and null when the field has opposite helicity. Because helicity is invariant under rotation, energy harvesting with the chiral structure is insensitive to polarization alignment.

To design the chiral response, we consider a subwavelength structure subject to a time-harmonic electromagnetic field with time dependency $e^{-i\omega t}$. In general, the induced electric and magnetic dipole moments $\mathbf{p}$ and $\mathbf{m}$ are given by

$$\begin{pmatrix} \mathbf{p} \\ \mathbf{m} \end{pmatrix} = \begin{pmatrix} \hat{\alpha}_e & -i\hat{\alpha}_c \\ i\hat{\alpha}_c & \hat{\alpha}_m \end{pmatrix} \begin{pmatrix} \mathbf{E} \\ \mathbf{H} \end{pmatrix}, \tag{1}$$

where $\hat{\alpha}_e$ is the electric polarizability, $\hat{\alpha}_m$ the magnetic polarizability, and $\hat{\alpha}_c$ the magnetoelectric cross polarizability. The form of the matrix is determined by reciprocity considerations. We describe the interaction of the structure with a *CP* field by rotating the electromagnetic field onto the Riemann-Silberstein basis $\mathbf{F}_\pm = (\mathbf{E} \pm i\eta\mathbf{H})/\sqrt{2}$, where η is the free-space impedance, and the dipole moments onto the combinations $\mathbf{d}_\pm = \sqrt{2}(\mathbf{p} \pm i\mathbf{m}/\eta)$, which radiate strictly right- or left-handed *CP* fields [15]. The resulting polarizability matrix is given by

$$\begin{pmatrix} \mathbf{d}_+ \\ \mathbf{d}_- \end{pmatrix} = \begin{pmatrix} \hat{\alpha}_e + \frac{\hat{\alpha}_m}{\eta^2} + \frac{2\hat{\alpha}_c}{\eta} & \hat{\alpha}_e - \frac{\hat{\alpha}_m}{\eta^2} \\ \hat{\alpha}_e - \frac{\hat{\alpha}_m}{\eta^2} & \hat{\alpha}_e + \frac{\hat{\alpha}_m}{\eta^2} - \frac{2\hat{\alpha}_c}{\eta} \end{pmatrix} \begin{pmatrix} \mathbf{F}_+ \\ \mathbf{F}_- \end{pmatrix}. \tag{2}$$

Equation (2) shows that the structure exhibits a differential response to right- and left-hand *CP* radiation when the cross polarizability is nonzero, with bias determined by the sign. This dissymmetry is maximized when

$$\hat{\alpha}_e = \frac{\hat{\alpha}_m}{\eta^2} = \pm\frac{\hat{\alpha}_c}{\eta}. \tag{3}$$

The first condition diagonalizes the polarizability matrix so that fields with different handedness are not mixed by scattering from the structure, while the second nulls the response to radiation of a particular handedness. As a consequence of reciprocity, minimizing the interaction with radiation of one handedness also maximizes interaction with radiation of the opposite handedness.

We now show that the chiral structure satisfying Eq. (3) exhibits enhanced performance in a *CP* field and orientation insensitivity in a LP field. The time-averaged power collected by the structure is given by

$$\langle P\rangle = \langle P_+\rangle + \langle P_-\rangle = \frac{\omega}{2}\mathrm{Im}\{\mathbf{F}_+^* \cdot \mathbf{d}_+ + \mathbf{F}_-^* \cdot \mathbf{d}_-\}. \tag{4}$$

We consider dyadic polarizability tensors for simplicity, denoting the structure axis by the unit vector $\mathbf{e}_0$ and the real and imaginary parts of the scalar polarizability by $\alpha = \alpha' + i\alpha''$. For a *CP* field, only one of the Riemann-Silberstein vectors is nonzero, and the collected power can be expanded using Eq. (2) and the identity $|\mathbf{F}_\pm \cdot \mathbf{e}_0|^2 = |\mathbf{F}_\pm|^2/2$ as

$$\langle P_{\mathrm{CP}}^\pm\rangle = \frac{\omega I_0}{2}\left(\frac{\alpha_e''}{2} + \frac{\alpha_m''}{2\eta^2} \pm \frac{\alpha_c''}{\eta}\right), \tag{5}$$

where $I_0 = |\mathbf{F}_\pm|^2$ is the incident power density. Applying Eq. (3) with the same choice of sign for the field helicity and the cross polarizability, the collected power is found to be twice the sum of the independent contributions from the independent electric and magnetic dipole moments with $\alpha_c'' = 0$. The opposite choice of sign, on the other hand, results in zero collected power, which is consistent with the null response. For a LP field, we have $\mathbf{F}_+ = \mathbf{F}_-^*$ and the incident field can be decomposed into left- and right-handed *CP* components with phase difference $e^{i2\theta}$. Denoting the power density as $I_0 = (|\mathbf{F}_+|^2 + |\mathbf{F}_-|^2)/2$, the collected power is given by

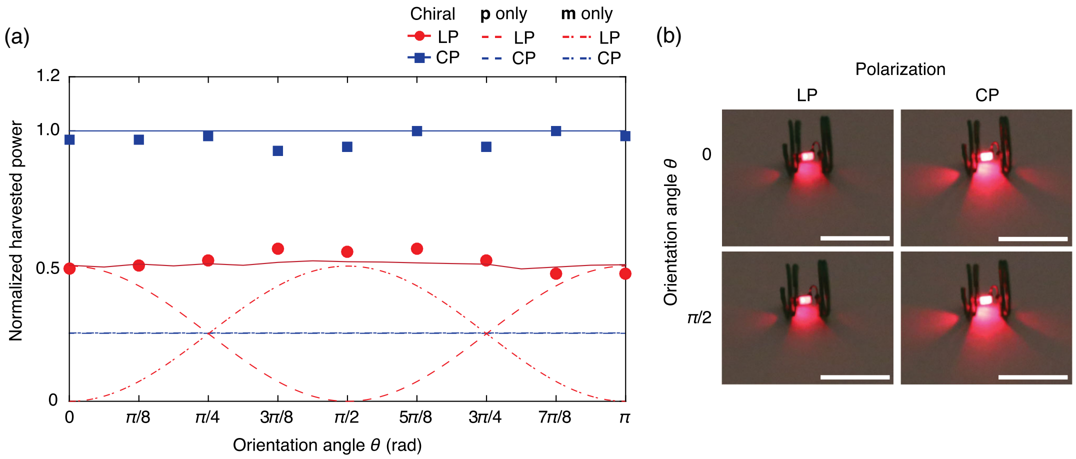

FIG. 2. Energy harvesting in a LP and *CP* field. (a) Simulated and measured variation in power harvested by a chiral structure in a LP and *CP* field as a function of θ. Both the structure and the *CP* field are left handed. Solid lines show simulations, markers experimental measurements, and dashed lines the theoretical power independently harvested by the structure's constituent electric dipole moment **p** and magnetic dipole moment **m**. (b) Image of the chiral structure in a LP and *CP* field with orientation $\theta = 0$ and $\theta = \pi/2$. Scale bar is 1 cm.

$$\langle P_{\rm LP}\rangle = \frac{\omega I_0}{2}\left[\frac{\alpha_e''}{2}(1+\cos 2\theta) + \frac{\alpha_m''}{2\eta^2}(1-\cos 2\theta)\right], \qquad (6)$$

which depends on θ but is independent of the field helicity. Remarkably, the dependency on θ is eliminated when Eq. (3) is satisfied. The performance in this case does not exhibit chiral enhancement, and the collected power is half that of the maximum in a *CP* field. The maximum power can be recovered by orienting **p** in the direction of **E** and **m** orthogonally in the transverse plane in the direction of **H**, such as in Ref. [23], although the resulting polarization response exhibits a dipolar dependency on θ.

III. RESULTS

To design a chiral structure satisfying Eq. (3), we begin with analytical approximations for the polarizability of a subwavelength helix (see Refs. [16,24]). Because the helix is constructed from a single conductor, the second condition in Eq. (3) is automatically satisfied when the first polarizability condition holds [16]. Using these dimensions as a starting point, we numerically simulate the power extracted by structure from a LP plane wave at normal incidence (CST Microwave Studio) and tune the diameter and height of the helix until the power collected from the 0 and $\pi/2$ orientations are equal (4 turns, 7-mm diameter, 7-mm length). We experimentally realize the structure by winding enameled copper wire and connecting the terminals of the wire to a circuit consisting of a rectifier (two-stage voltage doubler) and red light-emitting diode (LED), which enables energy harvesting to be visualized.

The incident field is generated by a cylindrical leaky cavity resonator ($f_0 = 1.5088$ GHz) in which the polarization state can be controlled by the tuning of the relative amplitude and phase of the signals exciting two orthogonal ports. A LP field is generated by driving the ports in phase and *CP* by applying equal amplitudes with a $\pi/2$ phase difference—the handedness is determined by the rotational direction of the phase difference. We place the chiral structure 14 cm (~0.7λ) above the cavity where the transverse components of the field have a measured impedance of $\eta = 378\ \Omega$, indicating that the field is predominantly radiative. The longitudinal component of the field is orthogonal to the structure axis and contributes negligibly to the power delivered to the load. We compare the harvested power by recording the LED intensity with a camera and calibrating the values by wirelessly powering the LED at different output power levels. This optical measurement scheme avoids the use of wire probes, which perturb the polarizabilities of the structure. Across all experiments, the power density of the incident field is normalized at the test position using a power probe.

Figure 2(a) shows the power collected by a left-handed chiral structure as function of orientation θ in a LP and left-hand *CP* field with a measured axial ratio of 0.912. By comparing the light intensity to a circuit directly powered by a network analyzer, the efficiency of power transfer to the structure in a LP field is estimated to be 0.5%. The transfer efficiency increases by a factor of 2 in the left-hand *CP* field of the same power density. In both cases, the power harvested is nearly uniform as the orientation is varied from 0 to π; the variation is measured to be 7.5% in the LP field and 16.1% in the *CP* field. The variation can be attributed to nonidealities in the chiral response and in the rotation apparatus used to vary the orientation. The orientation insensitivity and chiral enhancement of performance are visualized in Fig. 2(b) using the relative intensities of the LED.

We demonstrate helicity dependence in a *CP* field using chiral structures of opposite handedness. Figures 3(a)

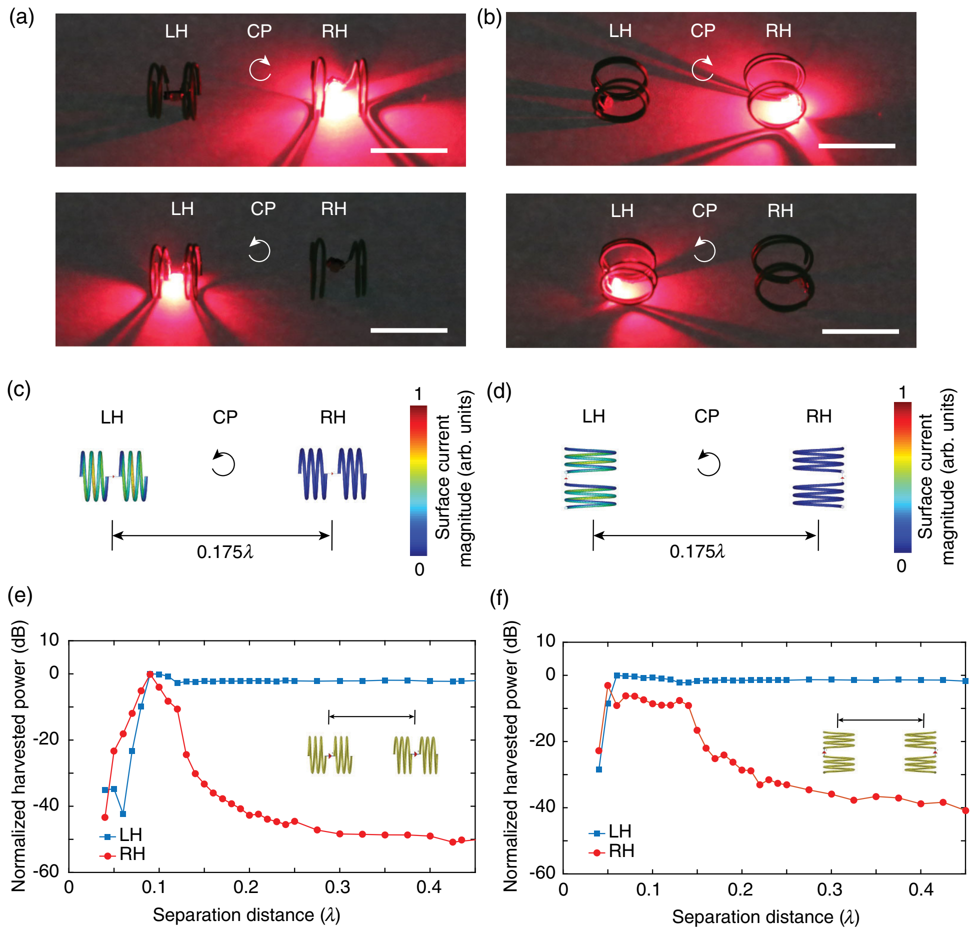

FIG. 3. Helicity dependence of the chiral structure. (a),(b) Image of (a) axially aligned and (b) axially parallel chiral structures of opposite handedness (LH, left-hand; RH, right-hand) in a *CP* field. (c),(d) Surface current on two (c) axially aligned and (d) axially parallel structures in a left-hand *CP* field. The distance between the coils is 35 mm (0.175λ). (e),(f) Power harvested by (e) axially aligned and (f) axially parallel structures of opposite handedness in a *CP* field as distance between the structures is varied. Scale bar is 1 cm.

and 3(b) show that the LEDs can be selectively activated by changing the handedness of the incident field while the power density incident on the structures is equal. Numerical simulations in Figs. 3(c) and 3(d) show that there is almost no current induced on the entire structure of handedness opposite to the incident field. For both the axially aligned and axially parallel structures, the separation distance between the two structures is deeply subwavelength (0.175λ). We numerically study the minimum distance at which the helicity selectivity is maintained. When axially aligned, the structures exhibit an isolation, defined as the ratio of the harvested power, of more than 20 dB for separation distances greater than 26 mm (0.13λ) [Fig. 3(e)]. The power harvested is approximately equal when the distance is less than 20 mm (0.1λ). In the axially parallel case, the isolation is less than 10 dB when separation is less than 28 mm (0.14λ), although weak isolation (> 5 dB) can be maintained as close as 12 mm (0.06λ) [Fig. 3(f)]. The loss in selectivity can be attributed to near-field effects between the two structures, which result in coupling between their dipole moments. The helicity selectivity enables the structures to be individually addressed through two independent polarization channels that do not depend on the orientation angle relative to the transmitter.

IV. CONCLUSION

We show that the chiral response of a single subwavelength structure can be engineered to enable a uniform collection of power from all orientations of an incident polarization state. Such chiral structures exhibit no dependency on the orientation θ in a LP field and provide enhanced performance in a *CP* field of the same handedness in which the collected power is twice that harvested by the constituent dipole moments. We describe the effect as a rotation of the polarization response on the Poincaré that exchanges the dependency on the orientation θ with a dependency on helicity χ which is invariant under rotation. In contrast to array-based techniques that combine direct-current power from multiple structures, the power collected by the chiral structure is delivered coherently to the electrical load, which enables fewer components and a more efficient operation of the harvesting circuit.

Although the chiral response eliminates dependency on the polarization orientation angle, the structure remains sensitive to the angle of incidence. An isotropic response can in principle be obtained with two orthogonally oriented chiral structures [17], although the overall volume would be approximately doubled without increasing the maximum power that can be collected. Incorporating such chiral structures into energy harvesting systems should enable miniaturization and more robust radiative powering of moving devices.

ACKNOWLEDGMENTS

This work was supported by a grant (NRF Fellowship) from the National Research Foundation, Singapore (Grant No. NRF-NRFF2017-7).

[1] W. C. Brown, The history of power transmission by radio waves, IEEE Trans. Microwave Theory Tech. **32**, 1230 (1984).

[2] J. A. Hagerty, F. B. Helmbrecht, W. H. McCalpin, R. Zane, and Z. B. Popovic, Recycling ambient microwave energy with broad-band rectenna arrays, IEEE Trans. Microwave Theory Tech. **52**, 1014 (2004).

[3] André Kurs, Aristeidis Karalis, Robert Moffatt, J. D. Joannopoulos, Peter Fisher, and Marin Soljačić, Wireless power transfer via strongly coupled magnetic resonances, Science **317**, 83 (2007).

[4] Omar M. Ramahi, Thamer S. Almoneef, Mohammed AlShareef, and Muhammed S. Boybay, Metamaterial particles for electromagnetic energy harvesting, Appl. Phys. Lett. **101**, 173903 (2012).

[5] Hubregt J. Visser and Ruud J. M. Vullers, RF energy harvesting and transport for wireless sensor network applications: Principles and requirements, Proc. IEEE **101**, 1410 (2013).

[6] Sangkil Kim, Rushi Vyas, Jo Bito, Kyriaki Niotaki, Ana Collado, Apostolos Georgiadis, and Manos M. Tentzeris, Ambient RF energy-harvesting technologies for self-sustainable standalone wireless sensor platforms, Proc. IEEE **102**, 1649 (2014).

[7] Babak Alavikia, Thamer S. Almoneef, and Omar M. Ramahi, Electromagnetic energy harvesting using complementary split-ring resonators, Appl. Phys. Lett. **104**, 163903 (2014).

[8] Thamer S. Almoneef and Omar M. Ramahi, Metamaterial electromagnetic energy harvester with near unity efficiency, Appl. Phys. Lett. **106**, 153902 (2015).

[9] Farrukh Mateen, Carsten Maedler, Shyamsunder Erramilli, and Pritiraj Mohanty, Wireless actuation of micromechanical resonators, Microsyst. Nanoeng. **2**, 16036 (2016).

[10] Hui-Teng Zhong, Xue-Xia Yang, Chong Tan, and Kai Yu, Triple-band polarization-insensitive and wide-angle metamaterial array for electromagnetic energy harvesting, Appl. Phys. Lett. **109**, 253904 (2016).

[11] Gabin T. Oumbé Tékam, Vincent Ginis, Jan Danckaert, and Philippe Tassin, Designing an efficient rectifying cut-wire metasurface for electromagnetic energy harvesting, Appl. Phys. Lett. **110**, 083901 (2017).

[12] Xuanming Zhang, Haixia Liu, and Long Li, Tri-band miniaturized wide-angle and polarization-insensitive metasurface for ambient energy harvesting, Appl. Phys. Lett. **111**, 071902 (2017).

[13] Sanghoek Kim, John S. Ho, and Ada S. Y. Poon, Midfield Wireless Powering of Subwavelength Autonomous Devices, Phys. Rev. Lett. **110**, 203905 (2013).

[14] Devansh R. Agrawal, Yuji Tanabe, Desen Weng, Andrew Ma, Stephanie Hsu, Song-Yan Liao, Zhe Zhen, Zi-Yi Zhu, Chuanbowen Sun, Zhenya Dong, Fengyuan Yang, Hung Fat Tse, Ada S. Y. Poon, and John S. Ho, Conformal phased surfaces for wireless powering of bioelectronic microdevices, Nat. Biomed. Eng. **1**, 0043 (2017).

[15] I. Fernandez-Corbaton, M. Fruhnert, and C. Rockstuhl, Objects of Maximum Electromagnetic Chirality, Phys. Rev. X **6**, 031013 (2016).

[16] Sergei A. Tretyakov, Frédéric Mariotte, Constantin R. Simovski, Tatiana G. Kharina, and Jean-Philippe Heliot, Analytical antenna model for chiral scatterers: Comparison with numerical and experimental data, IEEE Trans. Antennas Propag. **44**, 1006 (1996).

[17] Antti O. Karilainen and Sergei A. Tretyakov, Isotropic chiral objects with zero backscattering, IEEE Trans. Antennas Propag. **60**, 4449 (2012).

[18] V. S. Asadchy, I. A. Faniayeu, Y. Ra'di, S. A. Khakhomov, I. V. Semchenko, and S. A. Tretyakov, Broadband Reflectionless Metasheets: Frequency-Selective Transmission and Perfect Absorption, Phys. Rev. X **5**, 031005 (2015).

[19] Yiqiao Tang and Adam E. Cohen, Optical Chirality and Its Interaction with Matter, Phys. Rev. Lett. **104**, 163901 (2010).

[20] Y. Tang and A. E. Cohen, Enhanced enantioselectivity in excitation of chiral molecules by superchiral light, Science **332**, 333 (2011).

[21] Martin Schäferling, Daniel Dregely, Mario Hentschel, and Harald Giessen, Tailoring Enhanced Optical Chirality: Design Principles for Chiral Plasmonic Nanostructures, Phys. Rev. X **2**, 031010 (2012).

[22] Yang Zhao, Amir N. Askarpour, Liuyang Sun, Jinwei Shi, Xiaoqin Li, and Andrea Alu, Chirality detection of enantiomers using twisted optical metamaterials, Nat. Commun. **8**, 14180 (2017).

[23] Younes Ra'di and Sergei A Tretyakov, Balanced and optimal bianisotropic particles: Maximizing power extracted from electromagnetic fields, New J. Phys. **15**, 053008 (2013).

[24] H. A. Wheeler, A helical antenna for circular polarization, Proc. IRE **35**, 1484 (1947).